

SUPPLEMENTARY MATERIALS

On the nature of luminescence thermochromism of multinuclear copper(I) benzoate complexes in the crystalline state

Katarzyna N. Jarzembska,^{a,*} Michał Hapka,^a

Radosław Kamiński,^a Wojciech Bury,^b Sylwia E. Kutniewska,^a

Dariusz Szarejko,^a Małgorzata M. Szczęśniak ^c

^a Department of Chemistry, University of Warsaw, Żwirki i Wigury 101, 02-089 Warsaw, Poland

^b Department of Chemistry, University of Wrocław, Joliot-Curie 14, 50-383 Wrocław, Poland

^c Department of Chemistry, Oakland University, 146 Library Drive, Rochester, Michigan 48309-4479, United States

* Corresponding author: Katarzyna N. Jarzembska (katarzyna.jarzembska@gmail.com)

Table 1S. Selected X-ray data collection, processing and refinement parameters for all presented crystal structures.[#]

<i>Compound (temp.)</i>	Cu₄ (90 K)	Cu₄ (225 K)	Cu₄ (250 K)	Cu₄ (RT ^a)	Cu₆ (90 K)	Cu₆ (290 K)
Moiety formula	C ₂₈ H ₂₀ Cu ₄ O ₈	C ₂₈ H ₂₀ Cu ₄ O ₈	C ₂₈ H ₂₀ Cu ₄ O ₈	C ₂₈ H ₂₀ Cu ₄ O ₈	C ₄₂ H ₃₀ Cu ₆ O ₁₂	C ₄₂ H ₃₀ Cu ₆ O ₁₂
Moiety formula mass, <i>M_r</i> / a.u.	738.6	738.6	738.6	738.6	1108.0	1108.0
Crystal system	triclinic	triclinic	triclinic	triclinic	triclinic	triclinic
Space group	<i>P</i> 1 (no. 2)	<i>P</i> 1 (no. 2)				
<i>a</i> / Å	13.3196(17)	13.5990(2)	13.6438(9)	13.732(4)	9.1847(5)	11.364(3)
<i>b</i> / Å	14.9218(19)	15.0204(2)	15.0164(9)	15.061(4)	9.5452(5)	12.997(3)
<i>c</i> / Å	15.2602(19)	15.3847(3)	15.3876(10)	15.435(4)	11.2452(6)	13.734(3)
α / °	62.941(2)	62.454(2)	62.3347(12)	62.149(3)	107.4740(10)	95.647(4)
β / °	68.162(2)	67.6410(10)	67.5382(12)	67.493(4)	91.2090(10)	102.880(4)
γ / °	86.934(2)	87.5060(10)	87.5235(13)	87.584(4)	92.0990(10)	95.246(5)
<i>V</i> / Å ³	2482.5(5)	2542.99(9)	2545.5(3)	2570.7(11)	939.21(9)	1954.3(8)
<i>Z</i>	4	4	4	4	1	2
<i>T</i> / K	90	225	250	RT ^a	90	290
<i>F</i> ₀₀₀	1472	1472	1472	1472	552	1104
<i>d</i> _{calc} / g·cm ⁻³	1.976	1.929	1.927	1.909	1.959	1.883
θ range	1.63° – 33.65°	4.1° – 26.37°	1.55° – 33.87°	1.61° – 31.09°	1.9° – 33.58°	1.59° – 33.62°
Absorption coefficient, μ / mm ⁻¹	3.434	3.353	3.349	3.317	3.404	3.272
Crystal colour & shape	colourless rod	colourless rod	colourless rod	colourless rod	colourless chip	colourless chip
Crystal size / mm ³	0.14×0.04×0.03 ^b	0.14×0.08×0.07	0.14×0.04×0.03 ^b	0.38×0.13×0.09	0.06×0.06×0.05 ^c	0.06×0.06×0.05 ^c
No. of reflections collected / unique	36865 / 17744	46287 / 10361	39704 / 18670	44017 / 15208	14125 / 6757	29737 / 14142
<i>R</i> _{int}	3.50%	3.54%	2.91%	2.35%	2.33%	3.91%
No. of reflections with <i>I</i> > 3σ(<i>I</i>)	10787	7374	8071	9475	4940	5132
No. of parameters / constraints	721 / 160	721 / 160	721 / 160	721 / 160	271 / 60	541 / 120
<i>R</i> [<i>F</i>] (<i>I</i> > 3σ(<i>I</i>))	3.38%	2.85%	3.18%	3.11%	2.83%	3.75%
<i>wR</i> [<i>F</i> ²] (<i>I</i> > 3σ(<i>I</i>))	7.04%	6.04%	6.28%	7.50%	6.53%	7.47%
<i>R</i> [<i>F</i>] (all data)	7.63%	5.03%	10.87%	6.11%	5.04%	14.89%
<i>wR</i> [<i>F</i> ²] (all data)	8.16%	6.76%	7.84%	8.23%	7.18%	9.77%
<i>S</i> (<i>I</i> > 3σ(<i>I</i>))	1.27	1.29	1.17	1.71	1.42	1.22
<i>S</i> (all data)	1.43	1.39	1.46	2.00	1.53	1.61
$\rho_{\text{res}}^{\text{min/max}}$ / e·Å ⁻³	-1.00 / +0.63	-0.30 / +0.37	-0.56 / +0.49	-0.57 / +0.47	-0.68 / +0.53	-0.46 / +0.51
CCDC code	1878343	1878344	1878342	1878345	1878341	1878346

[#] All raw data are available under the following DOI: 10.18150/repod.0196712. ^a Room temperature. ^b Data sets measured on the same crystal. ^c Data sets measured on the same crystal.

Time-resolved Laue studies.

The time-resolved data sets were collected at the 14-ID beamline in the BioCARS station at the Advanced Photon Source (APS; Chicago, Illinois, USA) [34] at a 15 keV undulator setting (polychromatic radiation, $\lambda \approx 0.8 - 1.0 \text{ \AA}$), within the available beamtime (single X-ray pulse length of about 80 ps). Crystals were mounted on glass fibres using *Paratone N* oil or epoxy glue, for 90 K and 225 K data set collections, respectively. Optimal laser power was selected on the basis of preliminary short scans and the so-called correlation plot analysis [35]. The 90 K data sets were collected using the Nd:YAG/OPO nanosecond laser setup (OPOTEK Opolette 355 II HE; 7 ns pulse duration) with a 355 nm excitation wavelength and 5.6 ns pump-probe delay. In turn, the 225 K data sets were collected using a Ti:sapphire laser (Spectra-Physics Spitfire Pro laser coupled to a TOPAS optical parametric amplifier; 30 ps pulse duration) tuned to 360 nm with a pump-probe delay of 10 ns. The applied laser power varied within 0.7 – 1.8 mJ·mm⁻² per pulse for different measurements (depending on a crystal size and its reaction to a laser-light pulse, which was monitored via the spot-shape changes). To maximise the number of weak reflections observed in all data sets, the pump-probe cycle was repeated from 3 to 10 times for each frame before the detector read-out. Still frames were collected with an increment of 1° or 2°, preferably up to 180° rotation coverage (if the data collection was not interrupted due to crystal degradation). Light-ON and light-OFF frames were recorded in the prompt succession to minimise the effect of long-range fluctuations in the beam's position and/or intensity [36,37]. The light-ON/light-OFF pump-probe measurement was repeated 5 or 10 times for each angular setting to allow the subsequent statistical background estimation and filtering of the intensities. 6 and 9 data sets were measured for 90 K and 225 K temperatures, respectively. Raw data sets are available under the following DOI: 10.18150/repod.0196712.

Data processing pipeline is based on the so-called RATIO method [38,39]. In this approach the final result of the data reduction are the light-ON and light-OFF reflection intensity ratios ($R_o = I_o^{\text{ON}}/I_o^{\text{OFF}} = |F_o^{\text{ON}}|^2/|F_o^{\text{OFF}}|^2$), which are then used to estimate 'monochromatic' structure factor amplitudes not spurred by the wavelength dependence present in the original Laue diffraction data. The diffraction spot intensities from the Laue experiment were integrated with our new locally-written software [40], and later indexed by the modified version of the *LAUEUTIL* software package [41,42]. The used integration method, does not require any initial knowledge of the sample's cell dimensions and its orientation. After statistical analysis of the repeated light-ON/light-OFF pair measurements of each frame, ratios were averaged with the *SORTAV* program [43,44]. Finally, photodifference maps [45] were plotted based on the merged and scaled [46,47] data according to the following general equation:

$$\Delta\varrho_{\text{pdiff}}(\mathbf{r}) = \frac{1}{V} \sum_k (\sqrt{R_{o,k}} \cdot |F_{o,k}^{\text{mOFF}}| - |F_{o,k}^{\text{mOFF}}|) e^{i\phi_{c,k}^{\text{mOFF}}} e^{2\pi i \mathbf{h}_k \cdot \mathbf{r}}$$

where $R_{o,k}$ are synchrotron-derived intensity ratio values, $F_{o,k}^{\text{mOFF}}$ are the reference observed structure factors from the monochromatic light-OFF measurement, while $\phi_{c,k}^{\text{mOFF}}$ constitute the calculated structure factor phases from the same monochromatic data.

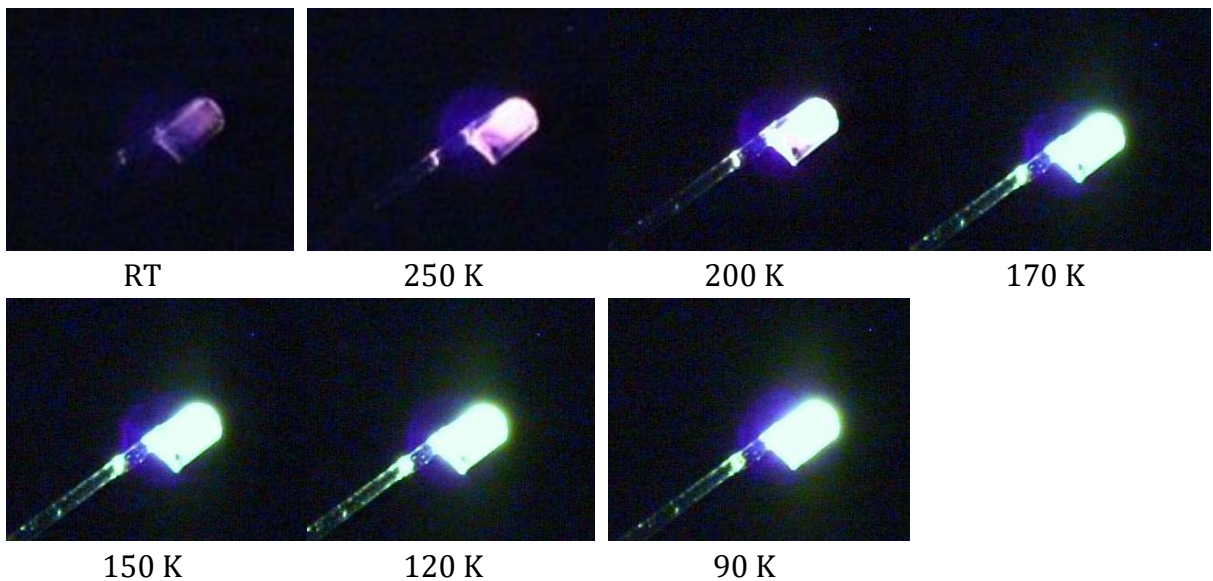


Figure 1S. Cu₄ complex single-crystal emission recorded with the diffractometer camera. The crystal is mounted on a goniometer head and irradiated with a 365 nm LED light through the focusing optics light-delivery assembly [48].

Table 2S. Comparison of selected ground (S_0) and excited triplet-state (T_1 & T_2) geometries. QM/MM denotes modelled solid-state structures; CAM-B3LYP and ω B97XD denote theoretical isolated-molecule results (shown only once for molecule A entries).

Molecule	Bond distance, $d / \text{\AA}$	Exp. (90 K)	QM/MM	QM/MM	ω B97XD	CAM-B3LYP	CAM-B3LYP	CAM-B3LYP
		S_0	S_0	T_1	S_0	S_0	T_1	T_2
A	Cu1-Cu3	2.7061(9)	2.735	2.438	2.740	2.738	2.498	2.665
	Cu1-Cu4	2.7335(7)	2.722	2.579	2.740	2.738*	2.498*	2.665*
	Cu2-Cu3	2.7129(7)	2.734	2.452	2.740	2.738*	2.498*	2.665*
	Cu2-Cu4	2.7325(9)	2.758	2.636	2.740	2.738*	2.498*	2.665*
	Cu1…Cu2 [¥]	2.8726(8)	2.846	2.608	2.932	2.911	2.623	2.372
	Cu3…Cu4 [‡]	4.622(1)	4.677	4.325	4.630	4.638	4.252	4.773
	Cu1-O1	1.867(1)	1.872	1.946	1.865	1.853	1.864	1.917
	Cu2-O8	1.876(1)	1.881	1.955	1.865	1.853*	1.864*	1.917*
	Cu3-O7	1.844(1)	1.843	1.874	1.857	1.844	1.852	1.932
	Cu4-O2	1.855(2)	1.851	1.841	1.857	1.844*	1.852*	1.932*
B	Cu5-Cu7	2.7256(9)	2.690	2.441	-	-	-	-
	Cu5-Cu8	2.7025(7)	2.704	2.524	-	-	-	-
	Cu6-Cu7	2.7118(7)	2.746	2.480	-	-	-	-
	Cu6-Cu8	2.7113(9)	2.732	2.547	-	-	-	-
	Cu5…Cu6 [¥]	3.0797(9)	3.128	2.724	-	-	-	-
	Cu7…Cu8 [‡]	4.4668(8)	4.445	4.188	-	-	-	-
	Cu5…O16	1.855(1)	1.854	1.907	-	-	-	-
	Cu6…O11	1.852(2)	1.853	1.933	-	-	-	-
	Cu7…O15	1.864(1)	1.868	1.892	-	-	-	-
	Cu8…O12	1.864(1)	1.865	1.859	-	-	-	-
Valence angle,		Exp. (90 K)	QM/MM	QM/MM	ω B97XD	CAM-B3LYP	CAM-B3LYP	CAM-B3LYP
$\theta / ^\circ$		S_0	S_0	T_1	S_0	S_0	T_1	T_2
A	Cu3-Cu1-Cu4	116.37(2)	117.97	119.10	115.31	115.77	116.65	127.15
	Cu3-Cu2-Cu4	116.17(2)	116.76	116.40	115.31	115.77	116.65	127.15
	Cu1-Cu3-Cu2	64.03(2)	62.71	64.46	64.69	64.23	63.35	52.85
	Cu1-Cu4-Cu2	63.41(2)	62.56	60.01	64.69	64.23	63.35	52.85
B	Cu7-Cu5-Cu8	110.75(2)	111.00	115.01	-	-	-	-
	Cu7-Cu6-Cu8	110.91(2)	108.47	112.80	-	-	-	-
	Cu5-Cu7-Cu6	69.00(2)	70.26	67.22	-	-	-	-
	Cu5-Cu8-Cu6	69.34(2)	70.27	64.97	-	-	-	-

[¥] Short diagonal. [‡] Long diagonal. * All bond are identical because the molecule is symmetric.

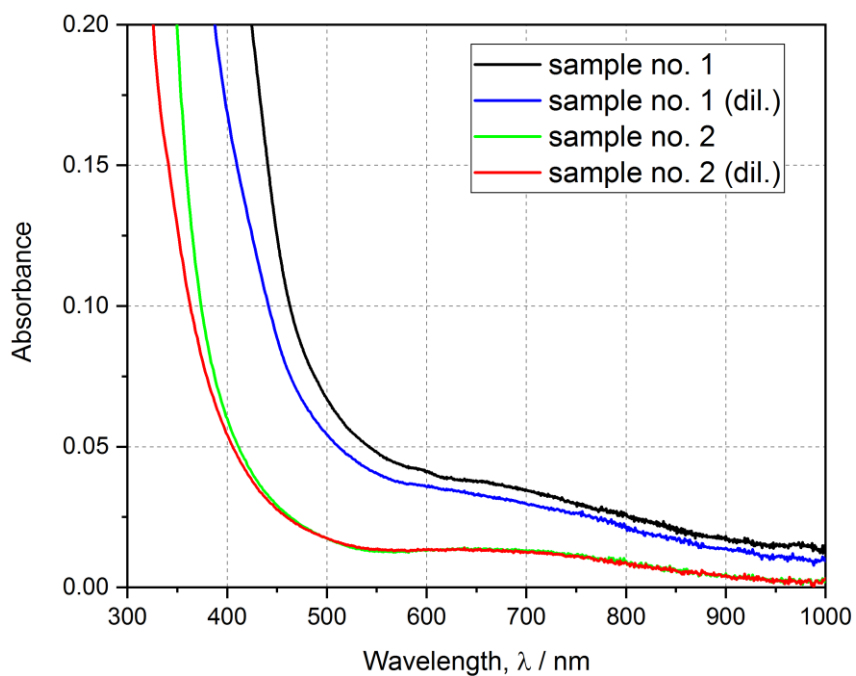
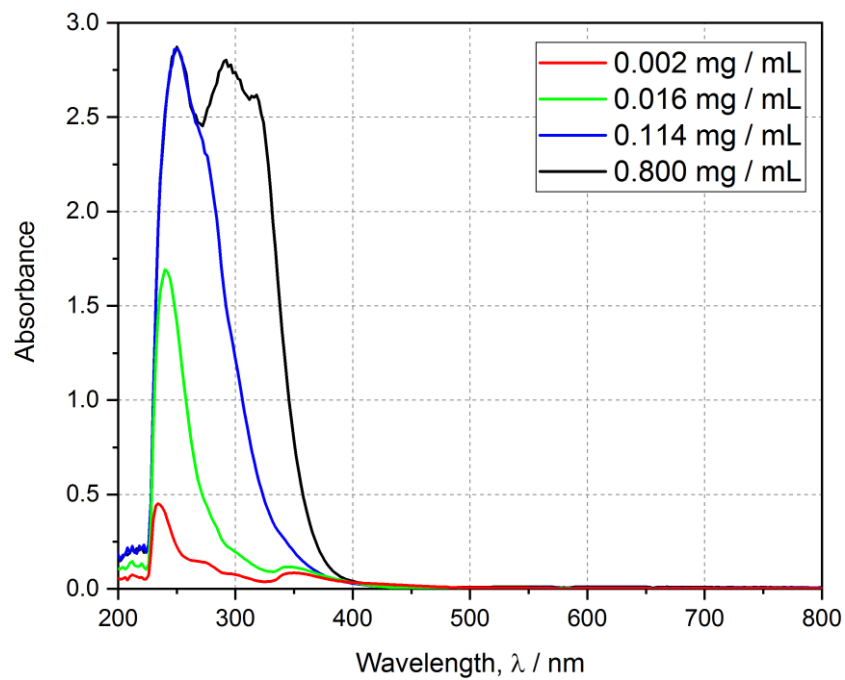


Figure 2S. UV-Vis solution absorption spectra collected for different concentrations of the Cu₄ complex in dichloromethane (top panel) and xylene (bottom panel; dil. = diluted).

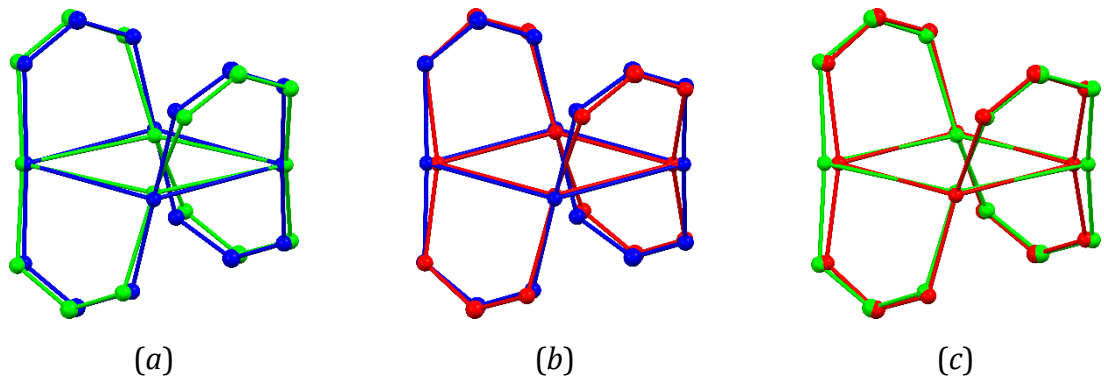


Figure 3S. Comparison of ground (S_0 : blue colour) and excited triplet-state (T_1 & T_2 : red & green colours, respectively) geometries from CAM-B3LYP isolated-molecule computations.

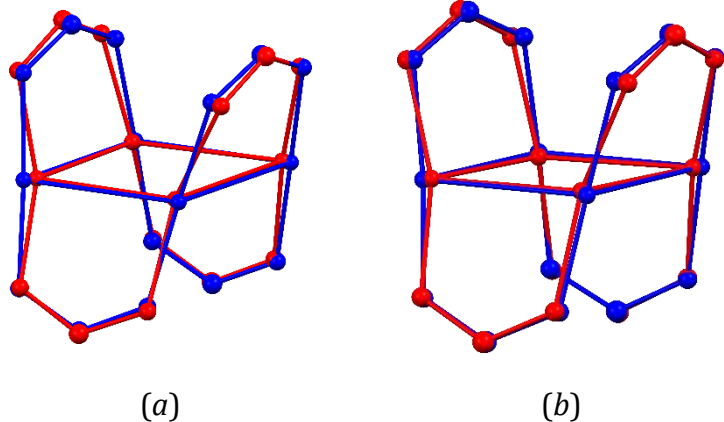


Figure 4S. Comparison of ground (S_0 : blue colour) and excited triplet-state (T_1 : red colour) geometries from QM/MM computations.

Table 3S. Excitation energies (dE) together with different density matrix based descriptors of the first ten triplet excited states of **Cu4**, computed at the CAM-B3LYP level of theory. PR_{NTO} defines the number of NTOs involved in the excitation.

<i>State</i>	dE / eV	Ω	PR	ω_{CT}	ω_{MC}	ω_{LC}	ω_{MLCT}	ω_{LMCT}	ω_{LLCT}	PR _{NTO}
1 ³ A	3.123	1.022	1.414	0.277	0.710	0.013	0.183	0.078	0.016	1.681
2 ³ B ₁	3.269	1.062	4.603	0.055	0.063	0.882	0.024	0.015	0.015	7.629
3 ³ B ₂	3.274	1.067	4.074	0.032	0.001	0.967	0.007	0.010	0.015	6.898
4 ³ A	3.284	1.068	4.066	0.024	0.001	0.975	0.007	0.007	0.010	7.291
5 ³ B ₃	3.284	1.068	4.059	0.024	0.000	0.976	0.007	0.007	0.010	7.270
6 ³ B ₁	3.322	1.023	1.634	0.233	0.668	0.100	0.161	0.060	0.012	1.778
7 ³ B ₂	3.549	1.017	1.307	0.227	0.765	0.008	0.149	0.069	0.008	2.102
8 ³ A	4.121	1.011	1.233	0.183	0.812	0.005	0.122	0.055	0.006	3.801
9 ³ B ₃	4.149	1.001	2.557	0.474	0.399	0.127	0.376	0.065	0.033	1.690
10 ³ B ₁	4.225	1.005	4.265	0.045	0.016	0.939	0.018	0.019	0.008	4.427

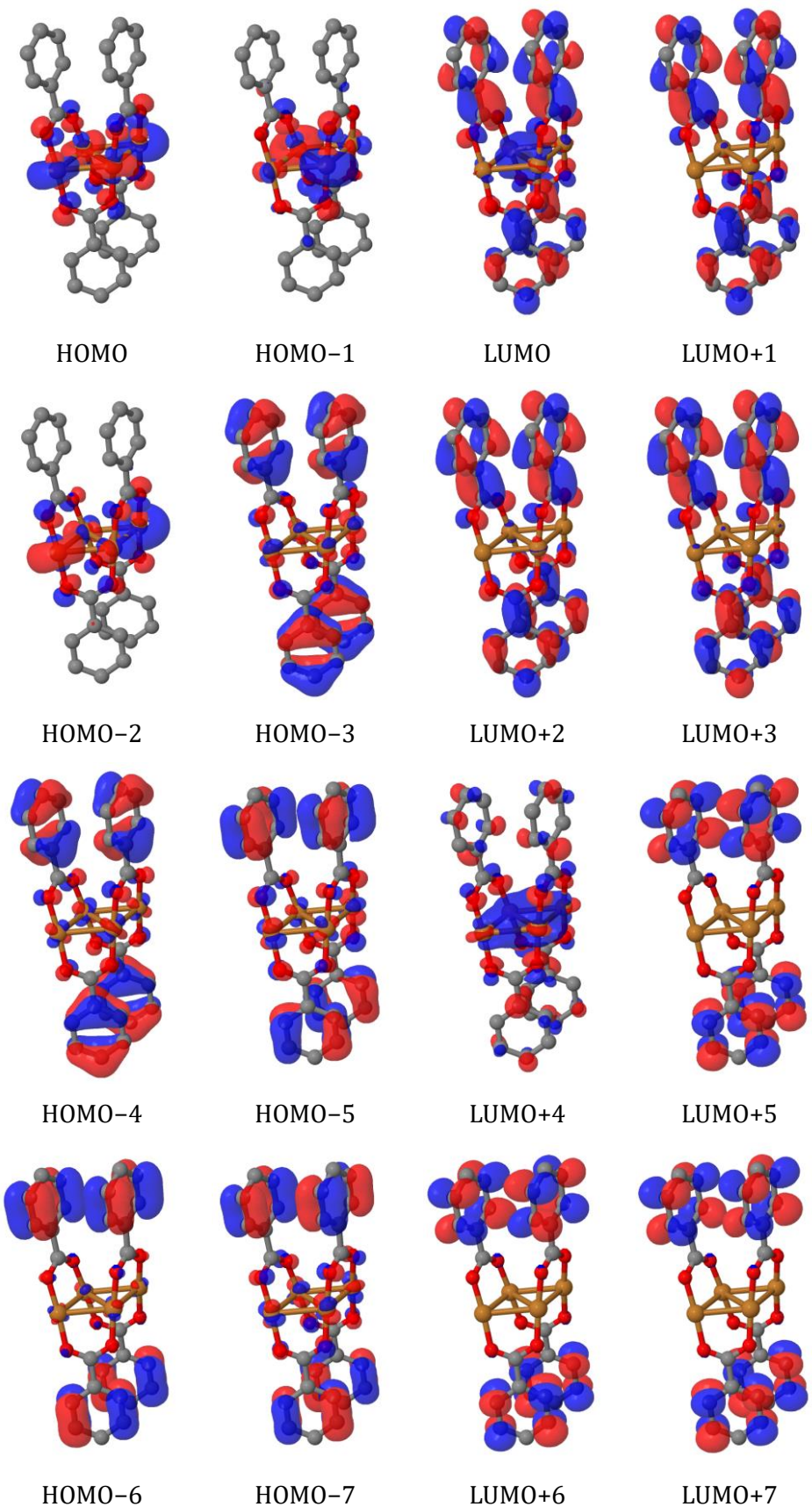


Figure 5S. Frontier molecular orbitals of the **Cu₄** complex (isosurfaces drawn at ± 0.04 a.u.; blue – positive; red – negative) obtained at the CAM-B3LYP/cc-pVDZ level of theory.

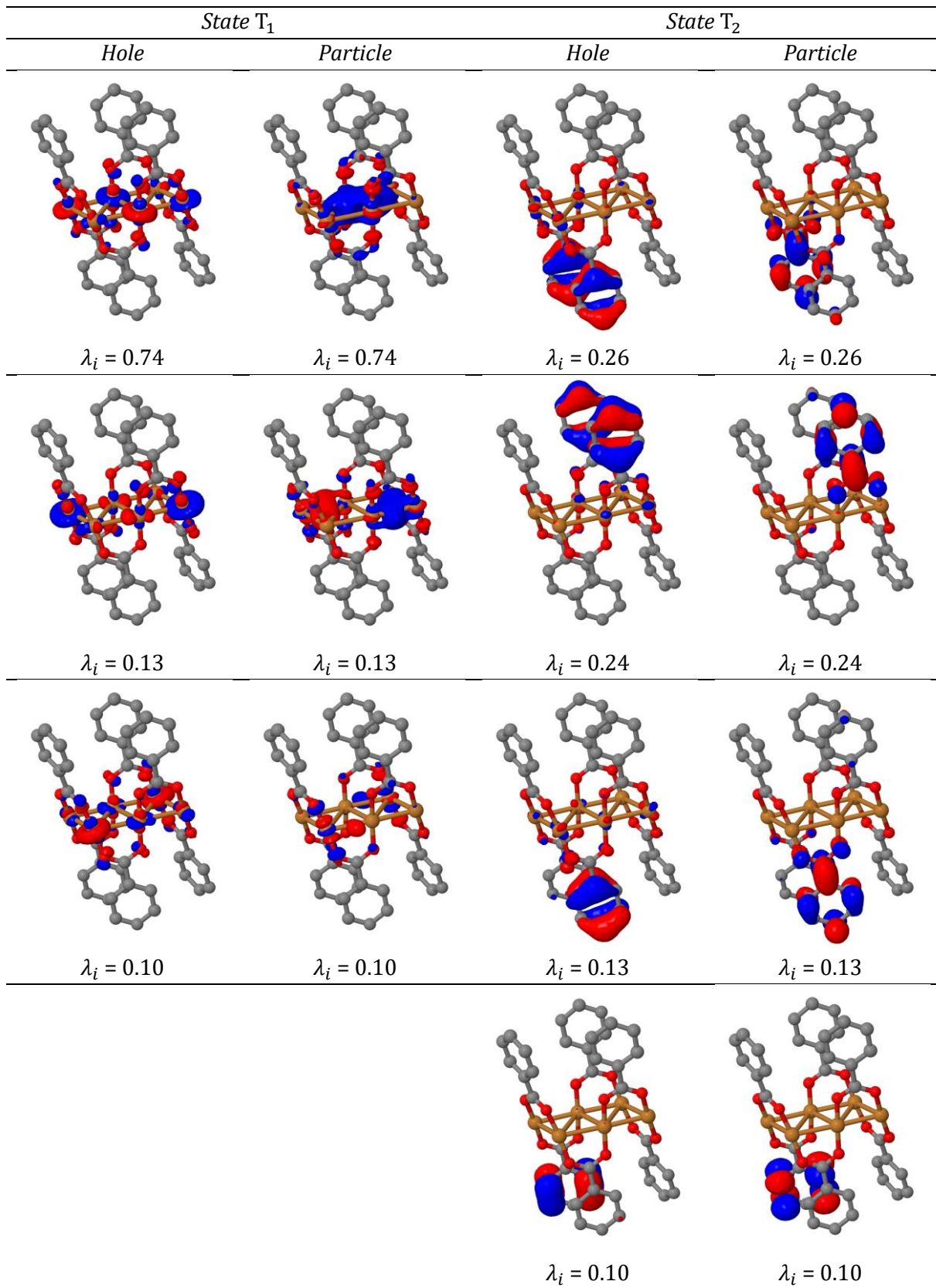


Figure 6S. Dominant hole and particle NTOs ($\lambda_i \geq 0.1$) for the T₁ and T₂ states of Cu6 (isosurfaces drawn at ± 0.04 a.u.; blue – positive; red – negative) obtained at the CAM-B3LYP/cc-pVDZ level of theory.

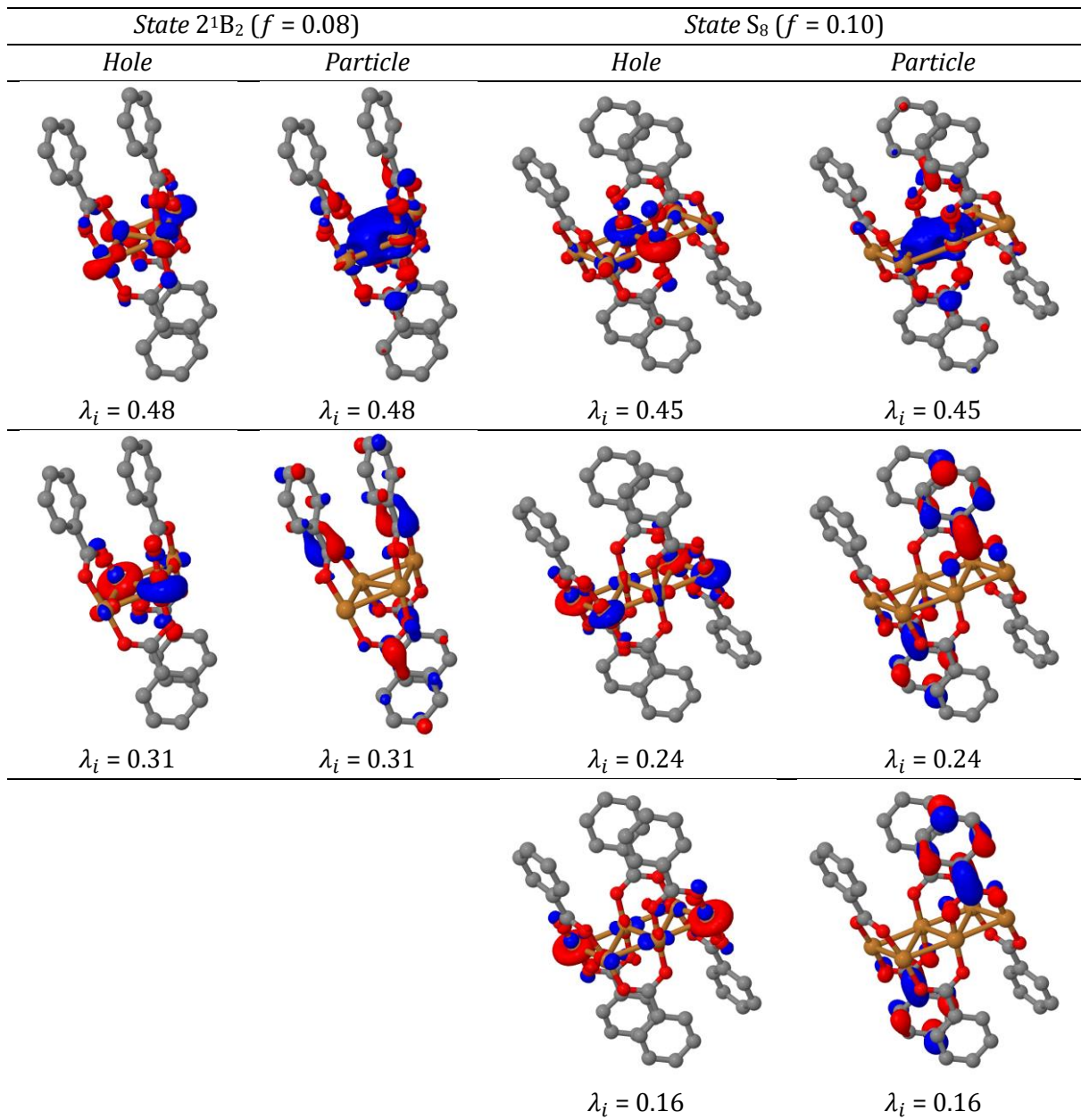


Figure 7S. Dominant hole and particle NTOs ($\lambda_i \geq 0.1$) for the 2^1B_2 and S_8 singlet states of **Cu₄** and **Cu₆** molecules, respectively (isosurfaces drawn at ± 0.04 a.u.; blue – positive; red – negative), obtained at the CAM-B3LYP/cc-pVDZ level of theory (f denotes oscillator strength).

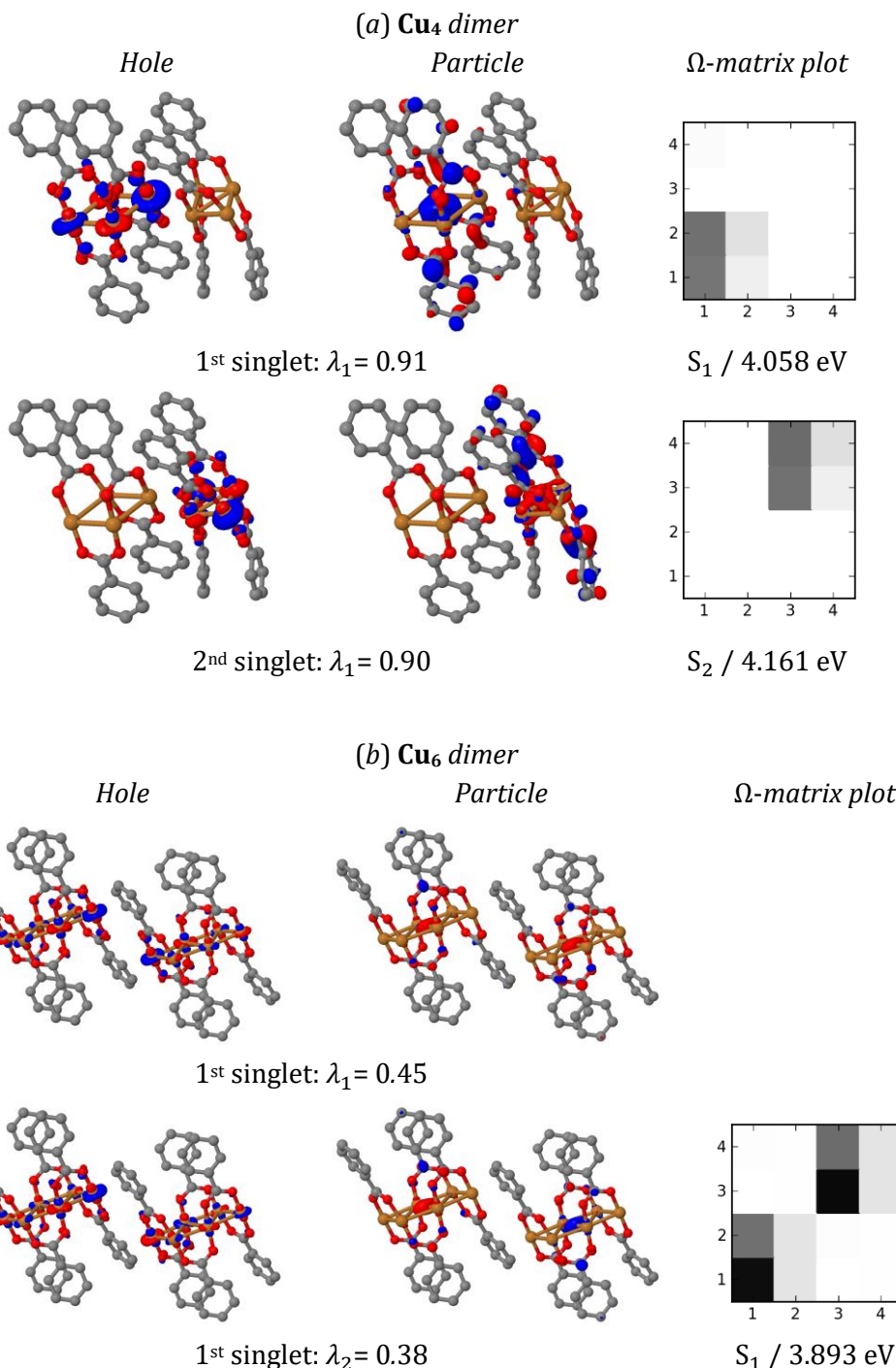


Figure 8S. Dominant NTO pairs and electron-hole correlation plots for S_1 and S_2 states of the **Cu₄** dimer (a) and S_1 state of the **Cu₆** dimer (b) (isosurfaces drawn at ± 0.04 a.u.; blue – positive; red – negative) obtained at the CAM-B3LYP/cc-pVDZ level of theory. Fragments 1 and 3 correspond to the Cu_n cores, whereas fragments 2 and 4 include all PhCO₂ ligands attached to the respective cores.

Figure 9S. $[(\text{PhCO}_2)_4\text{Cu}_4]$, singlet states, CAM-B3LYP, cc-pVDZ

Fragment 1: Cu4 core, fragments 2-5: PhCO₂ ligands

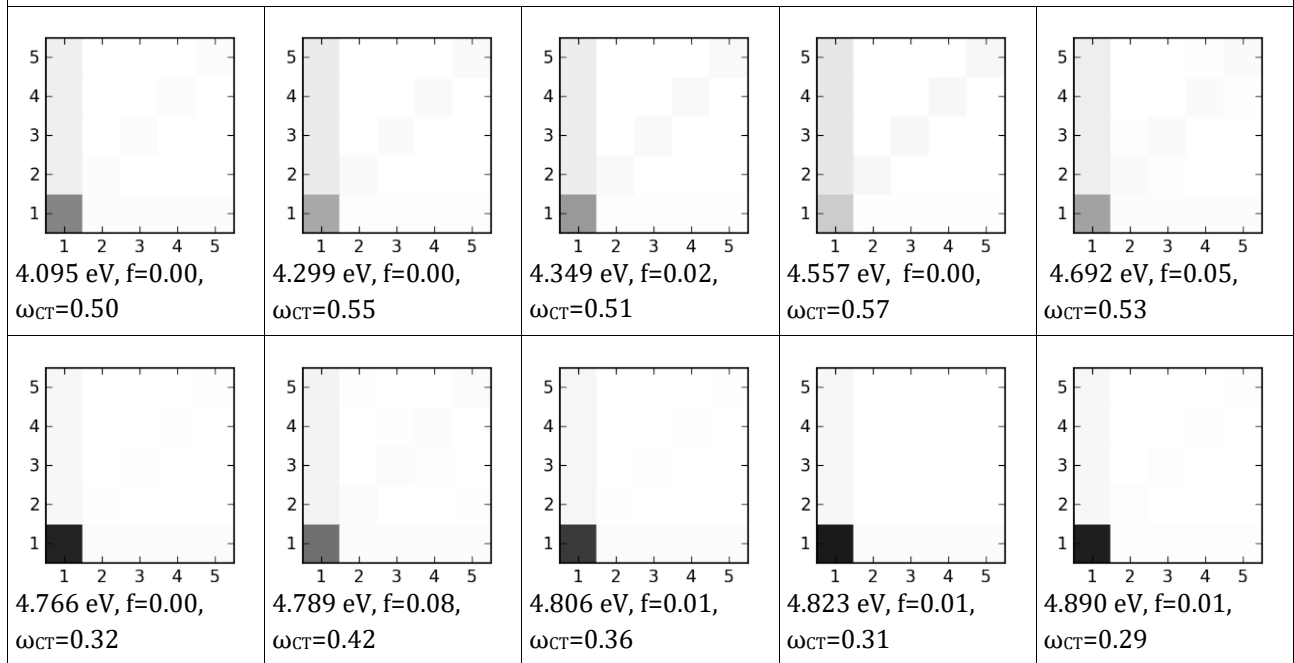


Figure 10S. $[(\text{PhCO}_2)_6\text{Cu}_6]$, singlet states, CAM-B3LYP, cc-pVDZ

Fragment 1: Cu6 core, fragments 2-7: PhCO₂ ligands

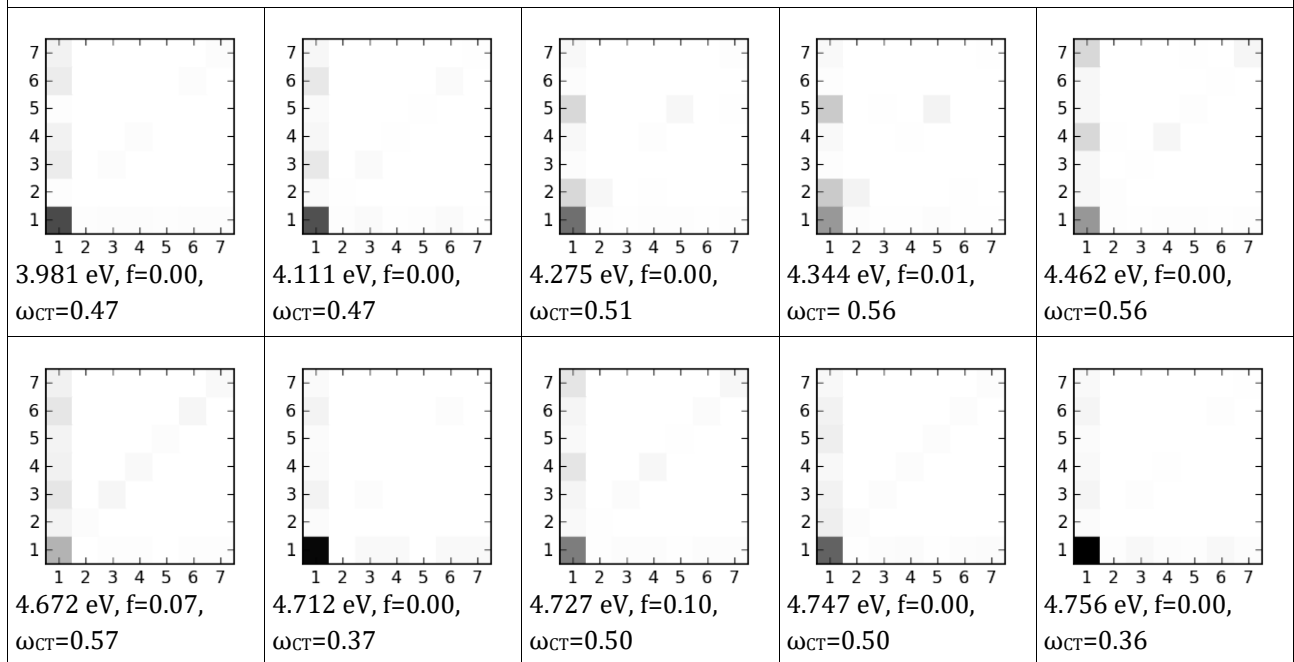


Table 4S. $[(\text{PhCO}_2)_4\text{Cu}_4]$, singlet states, CAM-B3LYP, cc-pVDZ

State	$\Delta E[\text{eV}]$	ω_{CT}	ω_{MC}	ω_{LC}	ω_{MLCT}	ω_{LMCT}	ω_{LLCT}	PR
1 ^1A	4.095	0.501	0.409	0.089	0.380	0.082	0.039	2.420
2 $^1\text{B}_3$	4.299	0.553	0.324	0.123	0.450	0.061	0.042	2.875
3 $^1\text{B}_1$	4.349	0.505	0.357	0.137	0.415	0.062	0.028	2.741
4 $^1\text{B}_2$	4.557	0.570	0.227	0.203	0.507	0.039	0.024	3.330
5 $^1\text{B}_1$	4.692	0.534	0.338	0.128	0.405	0.075	0.054	2.827
6 ^1A	4.766	0.324	0.645	0.031	0.194	0.105	0.026	1.570
7 $^1\text{B}_2$	4.789	0.423	0.465	0.112	0.296	0.080	0.047	2.276
8 $^1\text{B}_2$	4.806	0.360	0.596	0.043	0.237	0.096	0.027	1.707
9 $^1\text{B}_3$	4.823	0.313	0.666	0.022	0.193	0.096	0.024	1.514
10 $^1\text{B}_1$	4.890	0.290	0.655	0.055	0.198	0.068	0.024	1.605

Table 5S. $[(\text{PhCO}_2)_6\text{Cu}_6]$, singlet states, CAM-B3LYP, cc-pVDZ

State	$\Delta E[\text{eV}]$	ω_{CT}	ω_{MC}	ω_{LC}	ω_{MLCT}	ω_{LMCT}	ω_{LLCT}	PR
1	3.981	0.472	0.464	0.064	0.339	0.092	0.041	2.189
2	4.111	0.468	0.453	0.079	0.347	0.086	0.035	2.254
3	4.275	0.513	0.383	0.103	0.406	0.071	0.036	2.474
4	4.344	0.560	0.298	0.142	0.469	0.056	0.035	2.673
5	4.462	0.563	0.299	0.138	0.462	0.060	0.041	3.015
6	4.672	0.571	0.244	0.185	0.477	0.053	0.040	3.737
7	4.712	0.371	0.586	0.044	0.213	0.121	0.036	1.737
8	4.727	0.504	0.354	0.142	0.387	0.073	0.044	2.863
9	4.747	0.496	0.414	0.090	0.362	0.088	0.046	2.508
10	4.756	0.361	0.601	0.038	0.208	0.122	0.031	1.686

Figure 11S. [(PhCO₂)₄Cu₄], triplet states, CAM-B3LYP, cc-pVDZ

Fragment 1: Cu₄ core, fragments 2-5: PhCO₂ ligands

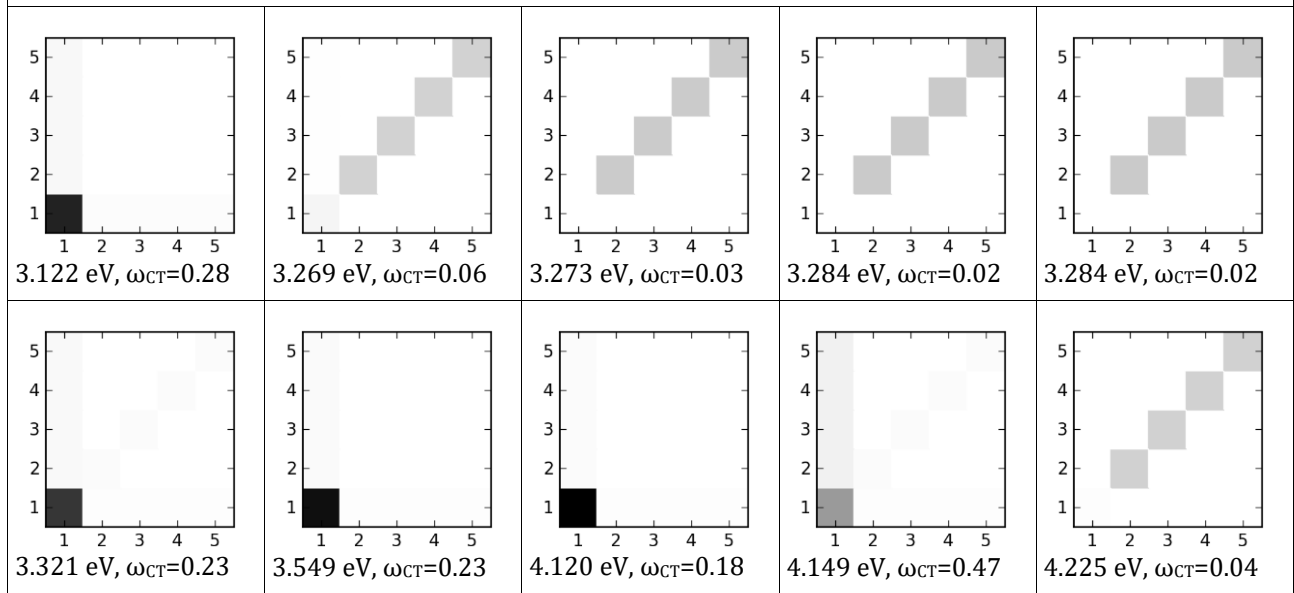


Figure 12S. [(PhCO₂)₆Cu₆], triplet states, CAM-B3LYP, cc-pVDZ

Fragment 1: Cu₆ core, fragments 2-7: PhCO₂ ligands

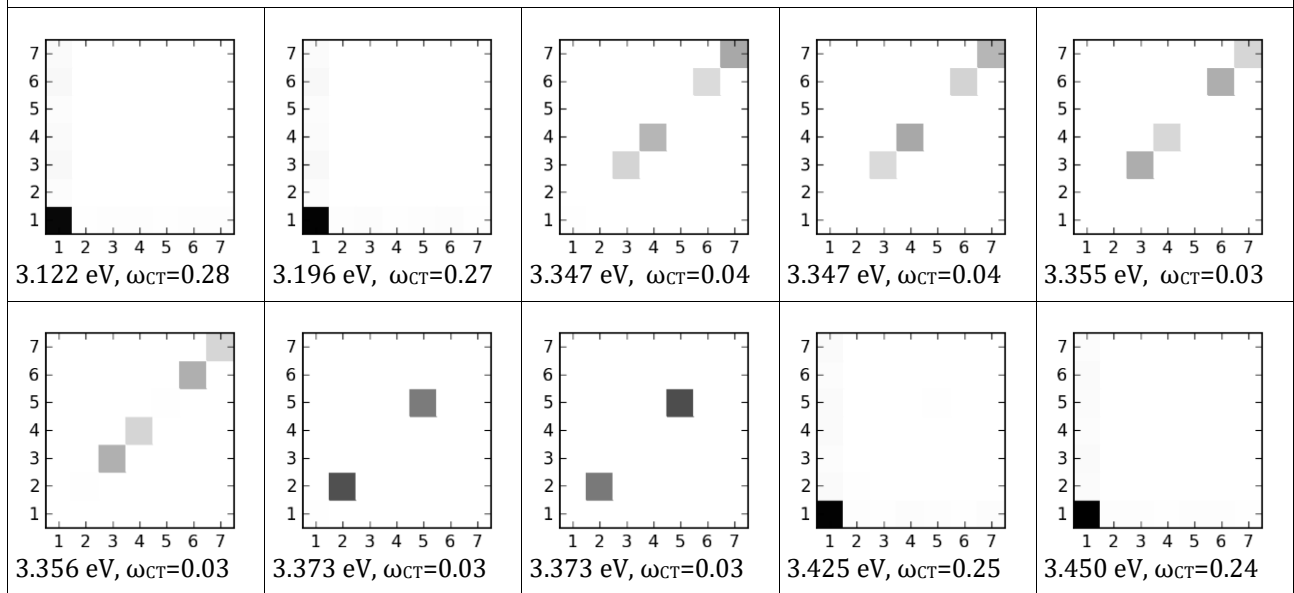


Table 6S. $[(\text{PhCO}_2)_4\text{Cu}_4]$, triplet states, CAM-B3LYP, cc-pVDZ

State	$\Delta E[\text{eV}]$	ω_{CT}	ω_{MC}	ω_{LC}	ω_{MLCT}	ω_{LMCT}	ω_{LLCT}	PR
1 ${}^3\text{A}$	3.122	0.277	0.710	0.013	0.183	0.078	0.016	1.414
2 ${}^3\text{B1}$	3.269	0.056	0.066	0.879	0.025	0.016	0.015	4.624
3 ${}^3\text{B2}$	3.273	0.032	0.001	0.967	0.007	0.010	0.015	4.074
4 ${}^3\text{A}$	3.284	0.024	0.001	0.975	0.007	0.007	0.010	4.066
5 ${}^3\text{B3}$	3.284	0.024	0.000	0.976	0.007	0.007	0.010	4.059
6 ${}^3\text{B1}$	3.321	0.232	0.664	0.104	0.160	0.060	0.012	1.648
7 ${}^3\text{B2}$	3.549	0.227	0.765	0.008	0.150	0.069	0.008	1.308
8 ${}^3\text{A}$	4.120	0.183	0.812	0.005	0.122	0.055	0.006	1.232
9 ${}^3\text{B3}$	4.149	0.474	0.399	0.127	0.376	0.065	0.033	2.556
10 ${}^3\text{B1}$	4.225	0.045	0.016	0.939	0.018	0.019	0.008	4.269

Table 7S. $[(\text{PhCO}_2)_6\text{Cu}_6]$, triplet states, CAM-B3LYP, cc-pVDZ

State	$\Delta E[\text{eV}]$	ω_{CT}	ω_{MC}	ω_{LC}	ω_{MLCT}	ω_{LMCT}	ω_{LLCT}	PR
1	3.122	0.280	0.710	0.010	0.181	0.083	0.017	1.413
2	3.196	0.267	0.721	0.012	0.174	0.078	0.014	1.395
3	3.347	0.038	0.008	0.954	0.009	0.011	0.017	3.926
4	3.347	0.035	0.003	0.961	0.008	0.011	0.017	3.905
5	3.355	0.028	0.001	0.971	0.007	0.008	0.013	3.927
6	3.356	0.028	0.002	0.970	0.007	0.008	0.013	3.996
7	3.373	0.032	0.007	0.962	0.009	0.008	0.014	2.125
8	3.373	0.030	0.003	0.966	0.008	0.008	0.014	2.086
9	3.425	0.254	0.725	0.021	0.163	0.077	0.013	1.399
10	3.450	0.244	0.734	0.022	0.164	0.068	0.012	1.388

Figure 13S. $[(\text{PhCO}_2)_4\text{Cu}_4]$, dimer, first 10 singlet states, CAM-B3LYP, cc-pVDZ

Fragments **1** and **3**: Cu4 cores, fragments **2** and **4**: all ligands attached to 1 and 3, respectively

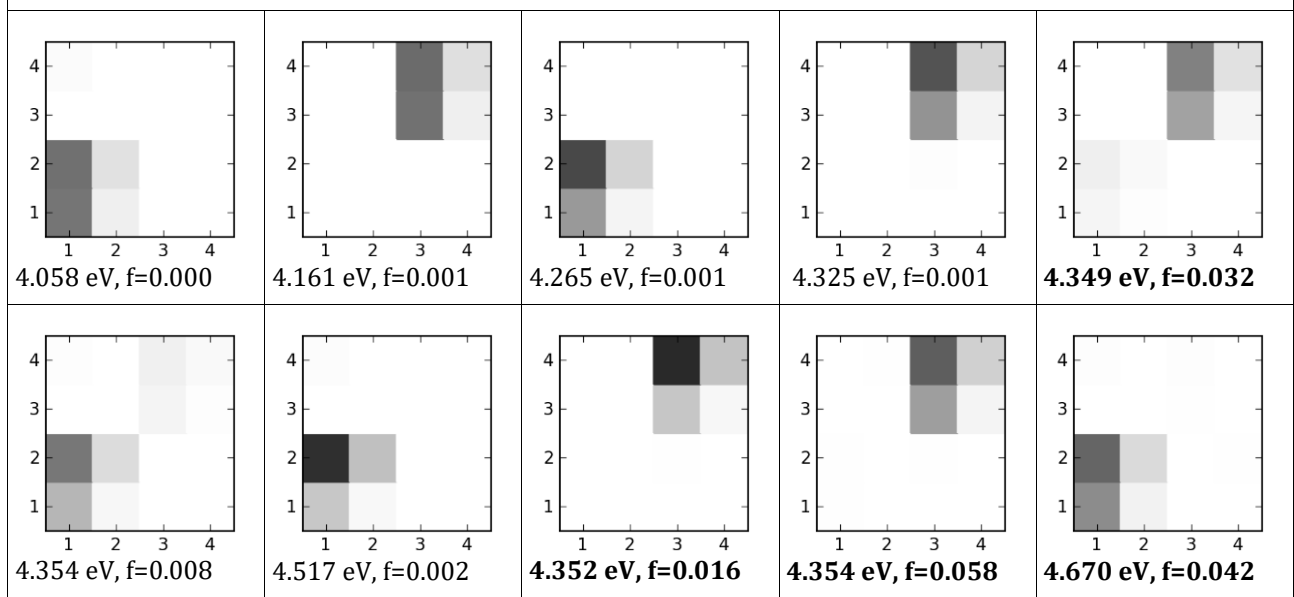


Figure 14S. $[(\text{PhCO}_2)_6\text{Cu}_6]$ dimer, first 10 singlet states, CAM-B3LYP, cc-pVDZ

Fragments **1** and **3**: Cu4 cores, fragments **2** and **4**: all ligands attached to 1 and 3, respectively

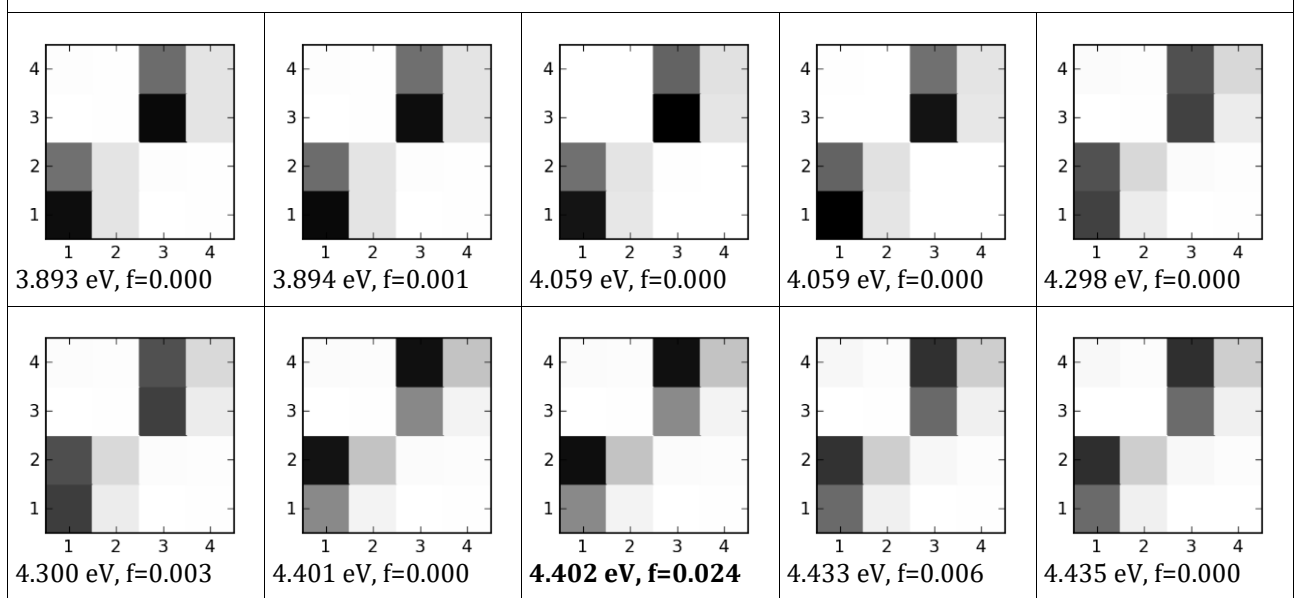


Table 8S. $[(\text{PhCO}_2)_4\text{Cu}_4]$, dimer, first 10 singlet states, CAM-B3LYP, cc-pVDZ

State	$\Delta E[\text{eV}]$	f	ω_{CT}	ω_{MC}	ω_{LC}	ω_{MLCT}	ω_{LMCT}	ω_{LLCT}
1	4.058	0.000	0.495	0.378	0.127	0.405	0.082	0.008
2	4.161	0.001	0.482	0.384	0.134	0.400	0.080	0.002
3	4.265	0.001	0.537	0.298	0.165	0.471	0.061	0.005
4	4.325	0.001	0.529	0.309	0.162	0.463	0.061	0.005
5	4.349	0.032	0.508	0.335	0.157	0.436	0.065	0.006
6	4.354	0.008	0.527	0.302	0.171	0.461	0.059	0.007
7	4.517	0.002	0.576	0.202	0.222	0.530	0.040	0.007
8	4.532	0.016	0.581	0.204	0.215	0.531	0.043	0.007
9	4.631	0.058	0.520	0.299	0.181	0.447	0.065	0.008
10	4.670	0.042	0.511	0.335	0.154	0.433	0.070	0.008

Table 9S. $[(\text{PhCO}_2)_6\text{Cu}_6]$, dimer, first 10 singlet states, CAM-B3LYP, cc-pVDZ

State	$\Delta E[\text{eV}]$	f	ω_{CT}	ω_{MC}	ω_{LC}	ω_{MLCT}	ω_{LMCT}	ω_{LLCT}
1	3.893	0.000	0.432	0.236	0.332	0.162	0.049	0.221
2	3.894	0.001	0.432	0.239	0.329	0.165	0.050	0.217
3	4.059	0.000	0.424	0.230	0.346	0.159	0.044	0.221
4	4.059	0.000	0.423	0.247	0.330	0.171	0.047	0.205
5	4.298	0.000	0.480	0.196	0.324	0.196	0.040	0.244
6	4.300	0.003	0.477	0.199	0.324	0.195	0.040	0.242
7	4.401	0.000	0.556	0.135	0.309	0.242	0.029	0.284
8	4.402	0.024	0.559	0.134	0.307	0.246	0.030	0.284
9	4.433	0.006	0.526	0.163	0.311	0.223	0.033	0.269
10	4.435	0.000	0.527	0.163	0.310	0.226	0.033	0.269

Figure 15S. $[(\text{PhCO}_2)_4\text{Cu}_4]$, dimer, first 10 triplet states, CAM-B3LYP, cc-pVDZ

Fragments **1** and **3**: Cu4 cores, fragments **2** and **4**: all ligands attached to 1 and 3, respectively

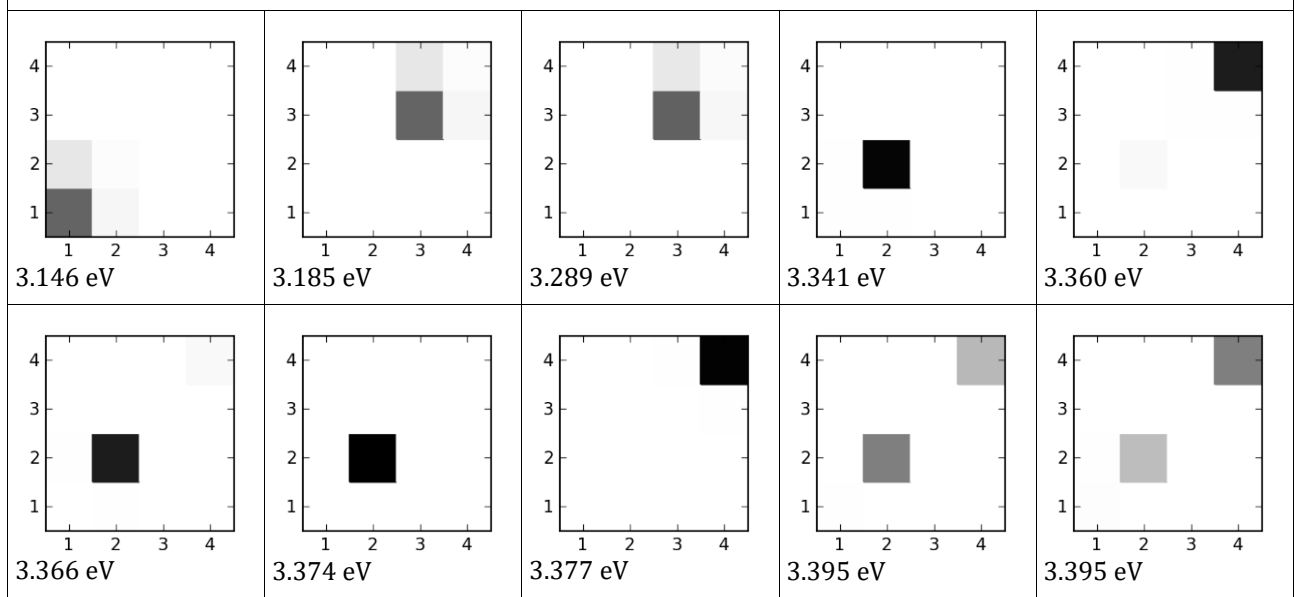


Figure 16S. $[(\text{PhCO}_2)_6\text{Cu}_6]$ dimer, first 10 triplet states, CAM-B3LYP, cc-pVDZ

Fragments **1** and **3**: Cu4 cores, fragments **2** and **4**: all ligands attached to 1 and 3, respectively

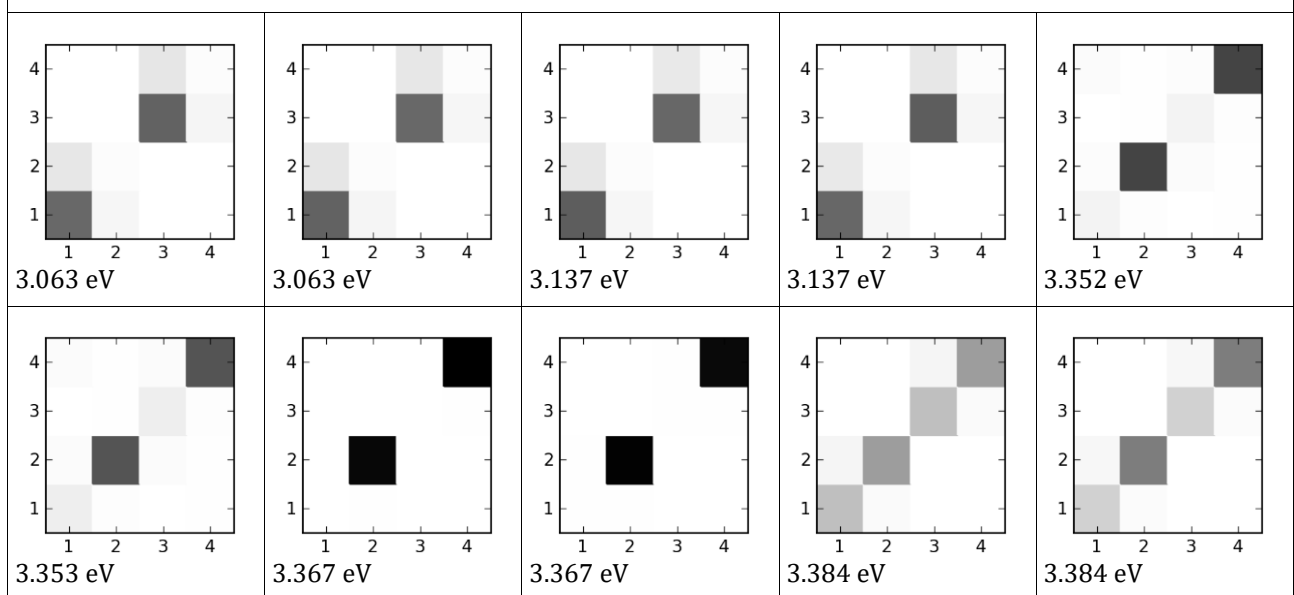


Table 10S. [(PhCO₂)₄Cu₄] dimer, first 10 triplet states, CAM-B3LYP, cc-pVDZ

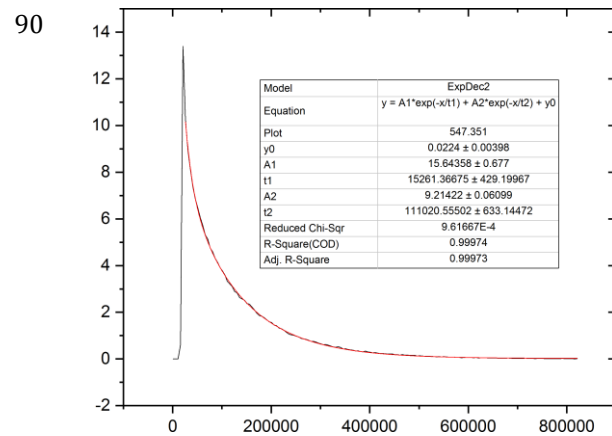
State	ΔE [eV]	ω_{CT}	ω_{MC}	ω_{LC}	ω_{MLCT}	ω_{LMCT}	ω_{LLCT}
1	3.146	0.271	0.700	0.029	0.184	0.085	0.001
2	3.185	0.269	0.700	0.031	0.184	0.083	0.001
3	3.289	0.251	0.711	0.038	0.177	0.073	0.002
4	3.341	0.023	0.009	0.967	0.011	0.011	0.001
5	3.360	0.043	0.010	0.947	0.016	0.019	0.009
6	3.366	0.042	0.008	0.951	0.016	0.016	0.009
7	3.374	0.016	0.001	0.982	0.008	0.007	0.001
8	3.377	0.020	0.003	0.976	0.009	0.009	0.003
9	3.395	0.029	0.011	0.960	0.012	0.012	0.005
10	3.395	0.035	0.020	0.946	0.016	0.014	0.005

Table 11S. [(PhCO₂)₆Cu₆] dimer, first 10 triplet states, CAM-B3LYP, cc-pVDZ

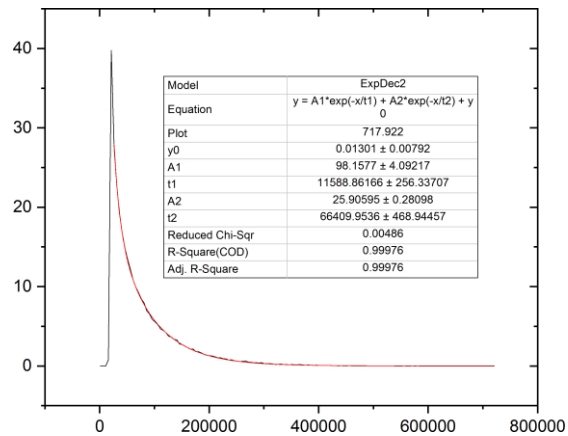
State	ΔE [eV]	ω_{CT}	ω_{MC}	ω_{LC}	ω_{MLCT}	ω_{LMCT}	ω_{LLCT}
1	3.063	0.273	0.343	0.384	0.091	0.043	0.140
2	3.063	0.274	0.355	0.371	0.094	0.045	0.135
3	3.137	0.263	0.365	0.372	0.092	0.043	0.128
4	3.137	0.262	0.346	0.391	0.087	0.040	0.136
5	3.352	0.112	0.051	0.837	0.033	0.016	0.063
6	3.354	0.120	0.068	0.811	0.037	0.017	0.066
7	3.367	0.019	0.001	0.980	0.004	0.005	0.010
8	3.367	0.021	0.005	0.975	0.005	0.005	0.010
9	3.384	0.142	0.186	0.672	0.047	0.024	0.072
10	3.385	0.116	0.144	0.740	0.037	0.020	0.059

T / K

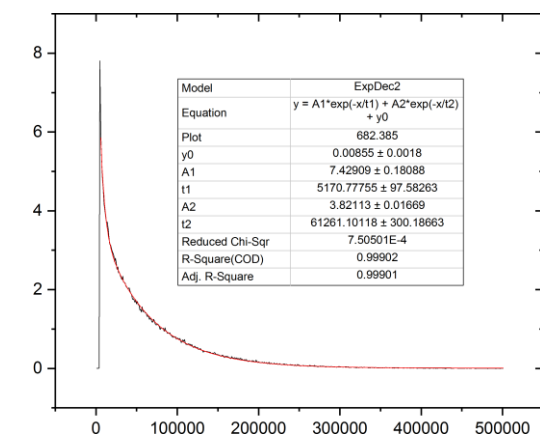
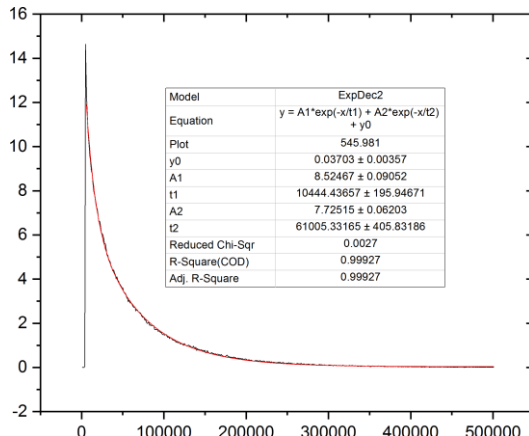
Green emission



Orange emission



150



200

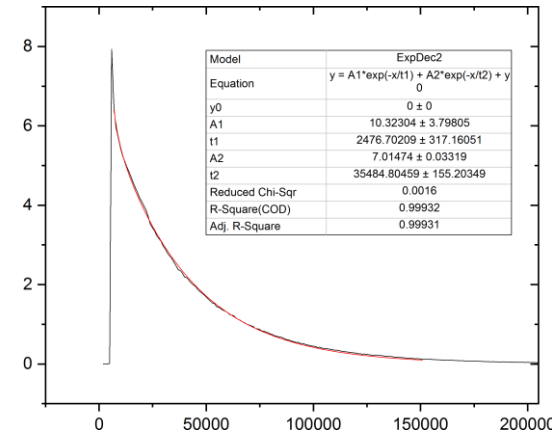
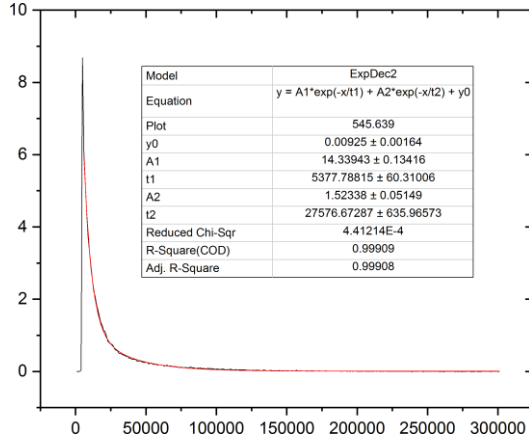


Figure 17S. Measured decay curves (black lines) and fitted exponential functions (red lines) for the Cu4 complex.

T / K

Green emission

Orange emission

250

RT

-

-

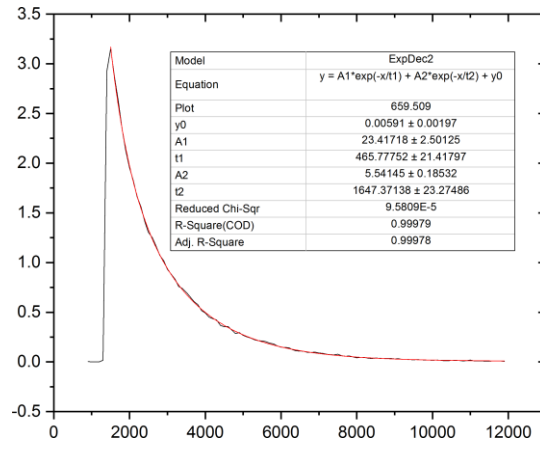
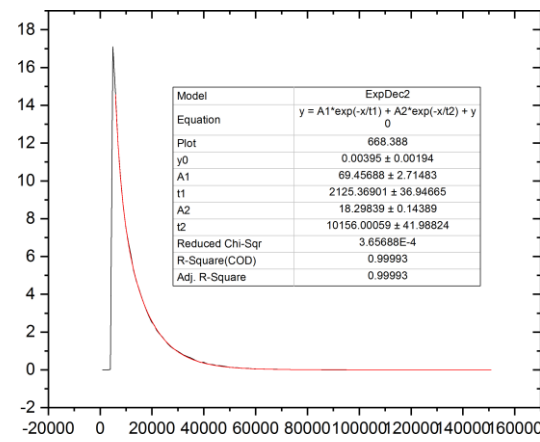


Figure 17S (continuation). Measured decay curves (black lines) and fitted exponential functions (red lines) for the **Cu₄** complex.

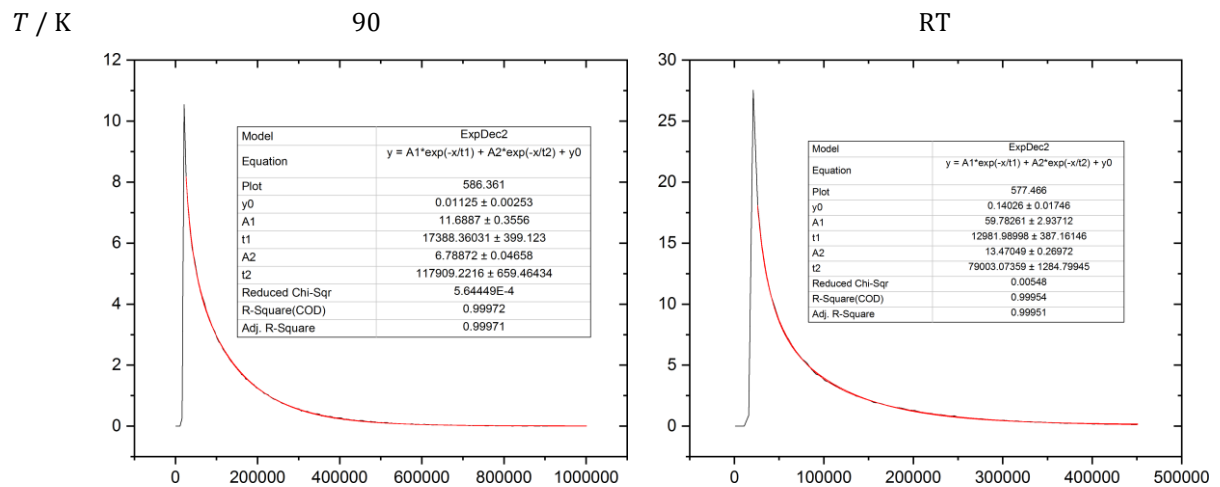


Figure 18S. Measured decay curves (black lines) and fitted exponential functions (red lines) for the Cu₆ complex.